



OPEN ACCESS

EDITED BY
Claudia Tanja Mierke,
Leipzig University, Germany

REVIEWED BY
Alessandra Fiorio Pla,
University of Turin, Italy
Madhumitha Rajagopal,
Mount Sinai Hospital, United States
Basilio Aristidis Kotsias,
University of Buenos Aires, Argentina

*CORRESPONDENCE
Ye Chun Ruan,
sharon.yc.ruan@polyu.edu.hk

[†]These authors have contributed equally
to this work

SPECIALTY SECTION

This article was submitted to Cell
Adhesion and Migration,
a section of the journal
Frontiers in Cell and Developmental
Biology

RECEIVED 23 September 2021

ACCEPTED 07 July 2022

PUBLISHED 30 August 2022

CITATION

Wuchu F, Ma X, Que Y, Chen J and
Ruan YC (2022), Biphasic regulation of
CFTR expression by ENaC in epithelial
cells: The involvement of Ca²⁺-
modulated cAMP production.
Front. Cell Dev. Biol. 10:781762.
doi: 10.3389/fcell.2022.781762

COPYRIGHT

© 2022 Wuchu, Ma, Que, Chen and
Ruan. This is an open-access article
distributed under the terms of the
[Creative Commons Attribution License
\(CC BY\)](https://creativecommons.org/licenses/by/4.0/). The use, distribution or
reproduction in other forums is
permitted, provided the original
author(s) and the copyright owner(s) are
credited and that the original
publication in this journal is cited, in
accordance with accepted academic
practice. No use, distribution or
reproduction is permitted which does
not comply with these terms.

Biphasic regulation of CFTR expression by ENaC in epithelial cells: The involvement of Ca²⁺-modulated cAMP production

Fulei Wuchu^{1†}, Xiyang Ma^{1†}, Yanting Que¹, Junjiang Chen^{1,2} and
Ye Chun Ruan^{1,3*}

¹Department of Biomedical Engineering, Faculty of Engineering, The Hong Kong Polytechnic University, Kowloon, Hong Kong SAR, China, ²Department of Physiology, Jinan University, Guangzhou, China, ³Shenzhen Research Institute, Hong Kong Polytechnic University, Shenzhen, China

The regulatory interaction between two typical epithelial ion channels, cystic fibrosis transmembrane conductance regulator (CFTR) and the epithelial sodium channel (ENaC), for epithelial homeostasis has been noted, although the underlying mechanisms remain unclear. Here, we report that in a human endometrial epithelial cell line (ISK), shRNA-based stable knockdown of ENaC produced a biphasic effect: a low (~23%) degree of ENaC knockdown resulted in significant increases in CFTR mRNA and protein levels, CFTR-mediated Cl⁻ transport activity as well as intracellular cAMP concentration, while a higher degree (~50%) of ENaC knockdown did not further increase but restored CFTR expression and cAMP levels. The basal intracellular Ca²⁺ level of ISK cells was lowered by ENaC knockdown or inhibition in a degree-dependent manner. BAPTA-AM, an intracellular Ca²⁺ chelator that lowers free Ca²⁺ concentration, elevated cAMP level and CFTR mRNA expression at a low (5 μM) but not a high (50 μM) dose, mimicking the biphasic effect of ENaC knockdown. Moreover, KH-7, a selective inhibitor of soluble adenylyl cyclase (sAC), abolished the CFTR upregulation induced by low-degree ENaC knockdown or Ca²⁺ chelation, suggesting the involvement of sAC-driven cAMP production in the positive regulation. A luciferase reporter to indicate CFTR transcription revealed that all tested degrees of ENaC knockdown/inhibition stimulated CFTR transcription in ISK cells, suggesting that the negative regulation on CFTR expression by the high-degree ENaC deficiency might occur at post-transcription stages. Additionally, similar biphasic effect of ENaC knockdown on CFTR expression was observed in a human bronchial epithelial cell line. Taken together, these results have revealed a previously unidentified biphasic regulatory role of ENaC in tuning CFTR expression involving Ca²⁺-modulated cAMP production, which may provide an efficient mechanism for dynamics and plasticity of the epithelial tissues in various physiological or pathological contexts.

KEYWORDS

the epithelial sodium channel (ENaC), cystic fibrosis transmembrane conductance regulator (CFTR), epithelial cells, endometrial epithelium, Ca²⁺, cAMP, sAC

Introduction

Fluid (electrolytes and water) secretion and absorption across the epithelium are two major physiological functions of epithelial cells, which are tightly regulated for the homeostasis of epithelial cell-enriched organ systems such as respiratory, digestive, urinary and reproductive tracts. Two typical epithelial ion channels, cystic fibrosis transmembrane conductance regulator (CFTR) and the epithelial sodium channel (ENaC), are broadly expressed and responsible for Cl^- secretion (Anderson et al., 1991) and Na^+ absorption (Palmer, 1992), respectively, driving water movement across the epithelium. The two channels are usually found in a reciprocal relationship (i.e. inversely related) (Berdiev et al., 2009), which is believed to maximize either epithelial secretion or absorption in the particular physiological context. For example, studies on the female reproductive system have shown that subject to hormonal changes over the estrus cycle in mice, uterine expression of CFTR is high at estrus phase (mid cycle in humans) and low at diestrus (late cycle in humans), while ENaC expression is, in the opposite way, low at estrus and high at diestrus (Chan et al., 2012). Such a cyclic expression pattern of these two channels is essential to the dominant uterine secretion to facilitate sperm transport at estrus, while uterine absorption to reduce luminal fluid and thus to stabilize embryo implantation at diestrus (Chan et al., 2009; Chen et al., 2012; Ruan et al., 2014).

The reciprocal relationship of CFTR and ENaC can result from hormonal regulation of their expression as observed in the female reproductive system (Ruan et al., 2014), although more studies have suggested that the two channels functionally inhibit each other (Chan et al., 2000; Konig et al., 2001), which could be through direct or indirect protein-protein interactions (Kunzelmann, 2001; Berdiev et al., 2007; Berdiev et al., 2009; Gentzsch et al., 2010). This is highlighted by the fact that Na^+ absorption is abnormally elevated in defective airways in cystic fibrosis (CF) (Hobbs et al., 2013), a common genetic disease caused by CFTR mutations. Amiloride, a selective ENaC pharmaceutical blocker, was therefore once proposed to be used as a potential drug for CF. However, clinical trials have failed to show the effectiveness of amiloride or its more potent analogue, benzamil, for CF (Graham et al., 1993; Pons et al., 2000; Hirsh et al., 2004). Moreover, CFTR and ENaC were found to be dependent on each other rather than inhibiting in sweat gland (Reddy et al., 1999; Reddy and Quinton, 2003). It is therefore suggested that the molecular and functional regulatory mechanism between the two channels is rather complex and may be far from being fully understood.

Interestingly, for the recent decade, both CFTR and ENaC have been shown to play an additional role beyond epithelial secretion/absorption, which is to regulate a number of cellular signaling pathways involving cAMP, Ca^{2+} , transcription factors, microRNAs and other signaling molecules for various physiological and pathological conditions (Chen et al., 2012;

Lu et al., 2012; Ruan et al., 2012; Ruan et al., 2014; Sun et al., 2014; Dong et al., 2015; Fei et al., 2018; Madacsy et al., 2018; Sun et al., 2018a; Sun et al., 2018b). Moreover, the expression of these two channels has been shown subject to regulation by cAMP or Ca^{2+} -dependent pathway (Dagenais et al., 2001; McCarthy and Harris, 2005; Dagenais et al., 2018). We therefore conducted the present study using endometrial epithelial cells as a model to understand if the modulation of ENaC would influence CFTR expression. To our surprise, the knockdown or inhibition of ENaC in endometrial epithelial cells resulted in a biphasic change of CFTR expression that is a low degree of ENaC deficiency upregulates CFTR, while further ENaC deficiency leads to downregulation of CFTR. We explored possible underlying mechanism and revealed the involvement of Ca^{2+} -modulated cAMP production in such regulation of CFTR by ENaC.

Results

Knockdown of ENaC results in biphasic change of CFTR expression in endometrial epithelial cells

To specifically modify ENaC, we adopted shRNA-based knockdown of ENaC α , the rate limiting subunit of ENaC (Canessa et al., 1994), in Ishikawa (ISK) cells, a commonly used human endometrial epithelial cell line (Nishida, 2002; Sun et al., 2018b). Three designs of shRNAs, shENaC α -1, -2 and -3 with predicated knockdown efficiency of 64%, 78% and 95% respectively were packaged in lentivirus and used to stably knock down ENaC in ISK cells. As a result, the mRNA level of ENaC α was reduced to $48 \pm 5\%$, $30 \pm 2\%$, and $27 \pm 2\%$ in cells treated with shENaC α -1, -2 and -3, respectively, as compared to the line with scrambled shRNAs as the negative control (shNC) (Figure 1A). We next used the ISK lines with shNC, shENaC α -1 and shENaC α -3 (ISK-shNC, ISK-shENaC α -1 and ISK-shENaC α -3) for subsequent experiments. Western blot results confirmed that ENaC α protein level was knocked down by about 50% and 70% in ISK-shENaC α -1 and ISK-shENaC α -3 cells, respectively, as compared to that in ISK-shNC (Figure 1B). To confirm that ENaC was functionally knocked down, we examined ENaC channel function by measuring the membrane potential (V_m) with a voltage-sensitive fluorescent dye, DiBAC4(3), which we previously published (Ruan et al., 2012). Results showed that in all these ISK lines, the addition of benzamil (10 μM) induced a decrease in DiBAC4(3) intensity indicating V_m hyperpolarization (Figure 1C), consistent with the known role of active ENaC in endometrial epithelial cells in mediating Na^+ influx and thus V_m depolarization. Such a benzamil-induced V_m hyperpolarization (indicating ENaC activity) was found to be reduced by about 23% and 50% in ISK-shENaC α -1 and ISK-shENaC α -3 lines, respectively, as compared to that in ISK-shNC (Figure 1C).

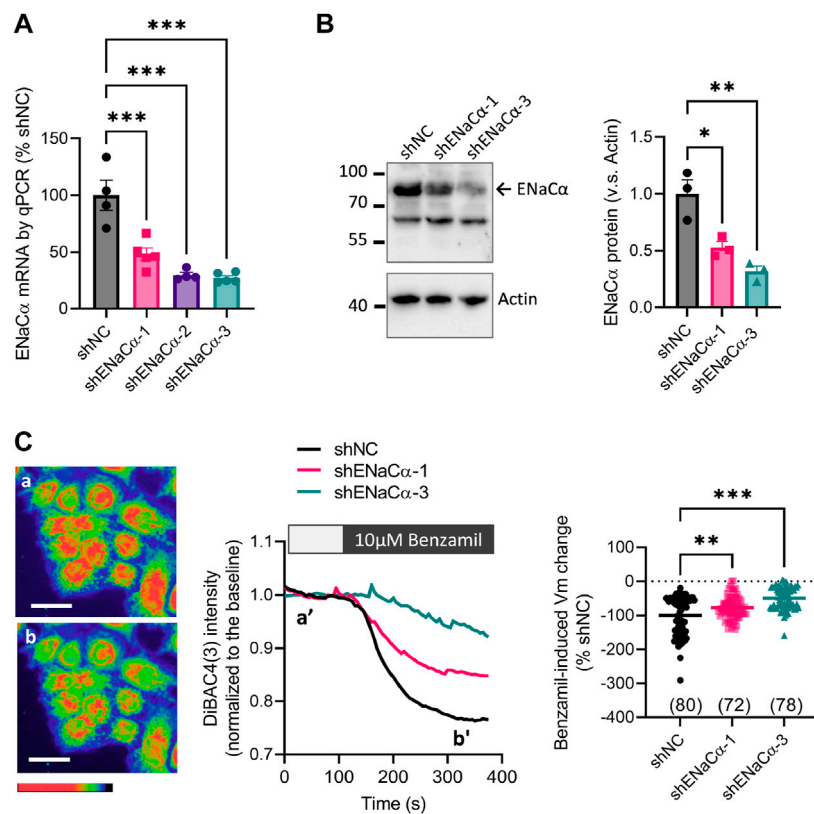


FIGURE 1

Different degrees of ENaC knockdown in ISK cells. (A–B) qPCR analysis of (A) and western blotting for (B) ENaCα in ISK cells with stable knockdown of ENaCα by transfection with lentivirus-packaged shRNAs against ENaCα (different designs: shENaCα-1, shENaCα-2 or shENaCα-3) or scrambled shRNAs as the negative control (shNC). (C) DiBAC4(3) measurement of membrane potential (V_m) with representative DiBAC4(3) fluorescent images (left), time-course traces of DiBAC4(3) intensity changes (middle), and quantifications (right) in the ISK lines treated with shNC, shENaC-1 or shENaC-3 before (a and a') and after (b and b') adding benzamil (10 μ M), a selective inhibitor of ENaC, into the bath. Pseudocolors in the images from red/yellow to blue/purple indicate V_m values from high to low. Scale bars = 50 μ m. $N = 4–5$ (A), 3 (B), and 72–80 (C). * $p < 0.05$, ** $p < 0.01$, *** $p < 0.001$, one-way ANOVA with *Dunnett post hoc* test.

In these ISK lines with a low (ISK-shENaCα-1, 23%) or high (ISK-shENaCα-3, 50%) degree of ENaC knockdown, we measured the expression of CFTR. Quantitative PCR (qPCR) results showed that the CFTR mRNA level in ISK-shENaCα-1 significantly increased by about 4 folds as compared to that in ISK-shNC (Figure 2A). However, in ISK-shENaCα-3 where ENaC was more knocked down, the mRNA level of CFTR did not further increase but was significantly lower than that in ISK-shENaCα-1 (Figure 2A). Consistently, only ISK-shENaCα-1 but not ISK-shENaCα-3 showed higher CFTR protein level compared to that in ISK-shNC (Figure 2B). We next examined Cl^- channel function of CFTR in the ISK lines by measuring intracellular Cl^- levels using a Cl^- -quenched fluorescent indicator, MQAE. While fluorescent intensity of MQAE was monitored under the microscope, a selective CFTR inhibitor, CFTRinh-172 (10 μ M) was added onto the cells. Upon the addition of CFTRinh-172, there was a drop of fluorescent signal indicating an increase of intracellular Cl^- concentration and thus suggesting CFTR function in mediating

Cl^- efflux in the cells (Figure 2C). Comparing these ISK lines, we found that ISK-shENaCα-1 exhibited a significantly larger CFTRinh-172-sensitive MQAE change compared to ISK-shNC (Figure 2C), indicating an increased gross CFTR activity in ISK-shENaCα-1. Whereas, in the ISK-shENaCα-3 with further ENaC knockdown, the CFTRinh172-sensitive change was similar compared to that in ISK-shNC, and significantly smaller than that in ISK-shENaCα-1 (Figure 2C). These results therefore consistently suggested that the regulation of CFTR by ENaC might be biphasic, i.e., CFTR upregulation by a low degree of ENaC deficiency but downregulation by further ENaC knockdown.

Involvement of cAMP in the regulation of CFTR by ENaC

We next asked how ENaC could regulate CFTR in such a biphasic manner. Since the promoter of CFTR gene is reported to

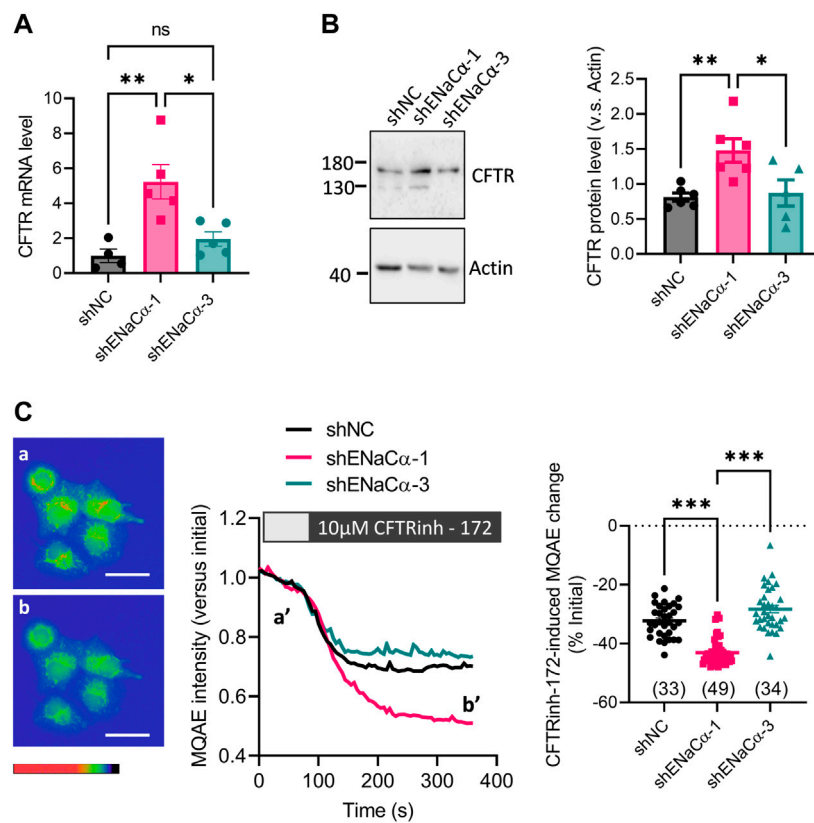


FIGURE 2

Effect of ENaC knockdown on CFTR expression in ISK cells. (A–B) qPCR (A) and representative western blot image with quantification (B) of CFTR in ISK cells treated with shNC, shENaC-1 or shENaC-3. (C) MAQE measurement of intracellular Cl⁻ concentration with representative MAQE fluorescent images (left), time-course traces (middle) and quantifications (right) in the ISK lines treated with shNC, shENaC-1 or shENaC-3 before (a and a') and after (b and b') the addition of CFTRinh-172 (10 μM), a selective inhibitor of CFTR. Pseudo-colors in the images from red/yellow to blue/purple indicate MAQE intensities (inversely correlated with Cl⁻ concentrations) from high to low. Scale bars = 50 μm N = 4–5 (A), 5–6 (B), and 33–49 (C). Ns: not significant. **p* < 0.05, ***p* < 0.01, ****p* < 0.001, one-way ANOVA with *Dunnett post hoc* test.

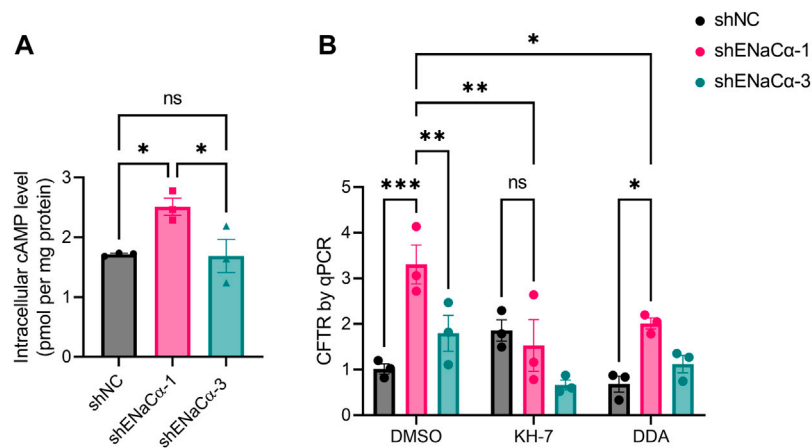
contain CRE element that is activated by cAMP response element binding protein (CREB) (Cheng et al., 1991; McCarthy and Harris, 2005), we tested possible involvement of cAMP. We measured the intracellular cAMP concentration of the ISK lines, which interestingly showed that, without any treatment, ISK-shENaCα-1 had a significantly higher basal level of intracellular cAMP (2.51 ± 0.14 pmol/mg) as compared to that of ISK-shNC (1.71 ± 0.02 pmol/mg) (Figure 3A). ISK-shENaCα-3 had a significantly lower basal level of cAMP (1.69 ± 0.27 pmol/mg) than that in ISK-shENaCα-1, which was not different with that in ISK-shNC. Therefore, the effect of ENaC knockdown on basal cAMP level in ISK cells was also biphasic.

We next treated the cells with drugs that inhibit cAMP production, 5-dideoxyadenosine (DDA), a selective inhibitor of transmembrane adenylyl cyclase (tmAC), and KH-7, a selective inhibitor of soluble adenylyl cyclase (sAC). Interestingly, in the presence of KH-7 (10 μM, 24 h), the biphasic effect of ENaC on CFTR mRNA levels was found completely reversed with the CFTR mRNA increase in ISK-

shENaCα-1 abolished (Figure 3B). However, although DDA (100 μM, 24 h) slightly lowered the CFTR mRNA level in all three ISK lines, the biphasic effect was not altered by DDA (Figure 3B). These results therefore suggested the involvement of sAC-mediated cAMP production in the regulation of CFTR by ENaC.

Involvement of intracellular Ca²⁺ in the regulation of CFTR by ENaC

sAC activity is well noted to be modulated by intracellular Ca²⁺ level (Jaiswal and Conti, 2003). We previously observed in endometrial epithelial cells that ENaC activity affected intracellular Ca²⁺ level (Ruan et al., 2012). We therefore wondered if the regulation of CFTR by ENaC could possibly be through Ca²⁺. We measured intracellular Ca²⁺ levels ([Ca²⁺]_i) in the ISK lines by Fura-2 imaging with calibration (Figure 4A), which showed that the basal [Ca²⁺]_i was significantly lower in

**FIGURE 3**

Involvement of cAMP in the regulation of CFTR expression by ENaC in ISK cells. **(A)** ELISA measurement of basal intracellular cAMP concentrations in the ISK lines treated with shNC, shENaC-1 or shENaC-3. Data were normalized to whole-cell protein levels. $N = 3$, ns: not significant. $*p < 0.05$, one-way ANOVA with *Dunnett post hoc* test. **(B)** qPCR analysis of CFTR mRNA levels in ISK lines treated with shNC, shENaC-1 or shENaC-3 after incubation with KH-7 (10 μ M, an inhibitor of sAC), DDA (100 μ M, an inhibitor of mACh), or DMSO as the control for 24 h. ns: not significant. $*p < 0.05$, $**p < 0.01$, $***p < 0.001$, two-way ANOVA with Tukey post hoc test.

ISK-shENaC α -1 (64.9 ± 2.8 nM) and ISK-shENaC α -3 (50.39 ± 1.9 nM), as compared to that in ISK-shNC (73.2 ± 3.0 nM) (Figure 4B). Consistently, the inhibition of ENaC by benzamil (0.1–10 μ M) induced reduction in $[Ca^{2+}]_i$ a dose-dependent manner, although the response to benzamil was reduced when ENaC was knocked down in ISK-shENaC α -1 and ISK-shENaC α -3 (Figure 4C). To mimic a situation of intracellular Ca^{2+} reduction, we treated the cells with BAPTA-AM, an intracellular Ca^{2+} chelator, which indeed produced decreases in $[Ca^{2+}]_i$ in ISK cells (Figure 4D). Interestingly, treating the cells with a low dose of BAPTA-AM (5 μ M) for 24 h increased CFTR mRNA expression as compared to the DMSO control, while at a higher dose of 50 μ M, it decreased mRNA CFTR expression in ISK cells (Figure 4E), mimicking the biphasic effect of ENaC knockdown. Similarly, intracellular cAMP level in ISK cells was found to be increased by the low dose (5 μ M, 1 h) of BAPTA-AM treatment, but lowered by the higher dose (50 μ M, 1 h), as compared to the control (Figure 4F). Moreover, the BAPTA-AM (5 μ M)-induced increase in CFTR mRNA level was reversed by treatment with KH-7 (10 μ M) and attenuated by DDA (10 μ M) (Figure 4G). These results therefore suggested the intracellular Ca^{2+} -modulated cAMP production underlying the regulation of CFTR by ENaC.

Effect of ENaC deficiency on CFTR transcription in ISK cells

To further understand the regulatory action of ENaC on CFTR expression, we adopted a dual luciferase reporter to

indicate the initiation of CFTR transcription in cells (see method). To our surprise, the reporter activity was found significantly higher in both ISK-shENaC α -1 and ISK-shENaC α -3, as compared to that in ISK-shNC, with no difference between ISK-shENaC α -1 and ISK-shENaC α -3 (Figure 5A), suggesting that CFTR transcription was stimulated with both degrees of ENaC knockdown. We then treated ISK cells with benzamil to inhibit ENaC, and found that benzamil at all doses tested (0.1–10 μ M, 24 h) enhanced the luciferase reporter activity in a dose-dependent manner (Figure 5B). However, we also measured CFTR mRNA in ISK cells by qPCR after the treatment with benzamil (0.1–10 μ M, 24 h), which showed that at 0.1 μ M benzamil slightly increased CFTR mRNA level, although at 10 μ M, it significantly decreased CFTR mRNA (Figure 5C). These results may suggest that inhibition of ENaC may at one hand stimulate CFTR transcription, while at the other hand affect CFTR mRNA maturation or stability.

Biphasic regulation of CFTR by ENaC in human bronchial epithelial cells

Having observed the relationship between CFTR and ENaC, we wondered whether this phenomenon was specific to ISK cells. We established ENaC knockdown model in a human bronchial epithelial cell line (HBE). Stable transfection of shENaC-1, -2 and -3 resulted in ENaC α expression reduction in HBE cells by about 44%, 34% and 65% respectively (Figure 6A). Only with the lowest

degree (34%) of ENaC knockdown (shENaC α -2) among the three, the mRNA expression of CFTR was found to be significantly increased compared to that in shNC-treated cells (Figure 6B). As ENaC was further knocked down (44%) by

shENaC α -1, the mRNA level of CFTR started to drop, which significantly decreased when ENaC was knocked down to a high degree (65%) by shENaC α -3 (Figure 6B). Therefore, a similar biphasic regulation of CFTR by ENaC was also seen in HBE cells.

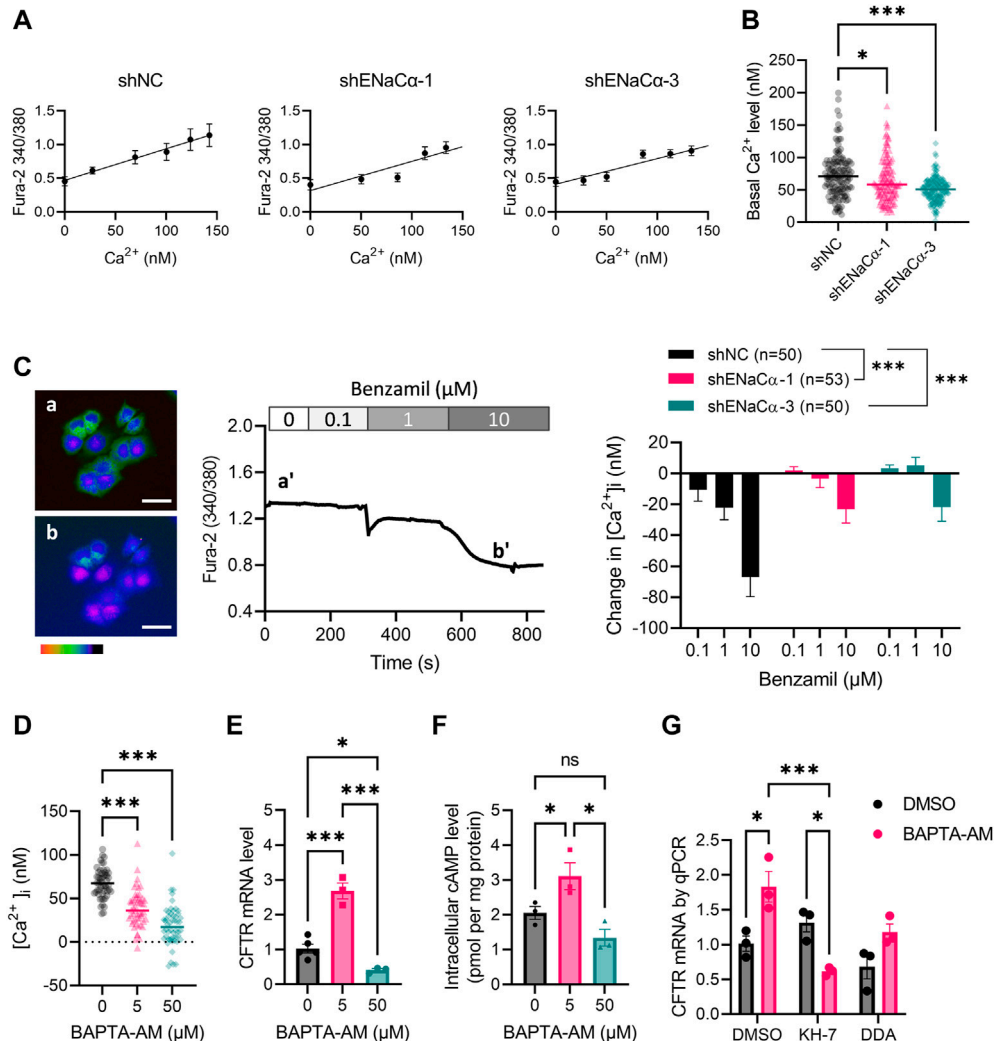


FIGURE 4

Involvement of intracellular Ca^{2+} in the regulation of CFTR expression by ENaC in ISK cells. **(A)** Intracellular Ca^{2+} concentrations ($[Ca^{2+}]_i$) of ISK lines with shNC, shENaC-1 or shENaC-3 were measured by Fura-2 imaging with calibration of Fura-2 intensity ratios at 340/380 nm into $[Ca^{2+}]_i$. **(B)** Basal $[Ca^{2+}]_i$ in the ISK lines were measured and calibrated accordingly. $N = 137-153$. $*p < 0.05$, $***p < 0.001$, one-way ANOVA with *Dunnett post hoc* test. **(C)** Representative Fura-2 ratio images of ISK cells with time-course traces showing the change in $[Ca^{2+}]_i$ before (a and a') and after (b and b') the addition of benzamil (0.1–10 μ M). Pseudo-colors in the images from red/yellow to blue/purple indicate Fura-2 340/380 ratios from high to low. Scale bars = 50 μ m. Quantification of the benzamil-induced change in $[Ca^{2+}]_i$ in ISK lines with shNC, shENaC-1 or shENaC-3 is shown on the right. N is shown for each group. $***p < 0.001$, two-way ANOVA. **(D)** $[Ca^{2+}]_i$ in ISK cells before (control) and after addition of BAPTA-AM (5–50 μ M), an intracellular Ca^{2+} chelator. **(E)** qPCR analysis of CFTR mRNA levels in ISK cells treated with BAPTA-AM at 5 μ M for 24 h or at 50 μ M for 30 min. $N = 3$. $*p < 0.05$, $***p < 0.001$, one-way ANOVA with *Dunnett post hoc* test. **(F)** ELISA measurement of intracellular cAMP in ISK cells after 1 h treatment with BAPTA-AM (5–50 μ M) or DMSO as control in the presence of IBMX (100 μ M). $N = 3$. *Ns*: not significant. $*p < 0.05$, one-way ANOVA with Newman-Keuls multiple comparisons test. **(G)** qPCR analysis of CFTR mRNA levels in ISK cells 24 h after treated with BAPTA-AM (5 μ M), KH-7 (10 μ M), DDA (100 μ M) or DMSO. $N = 3$. $*p < 0.05$, $***p < 0.001$, two-way ANOVA with *Tukey post hoc* test.

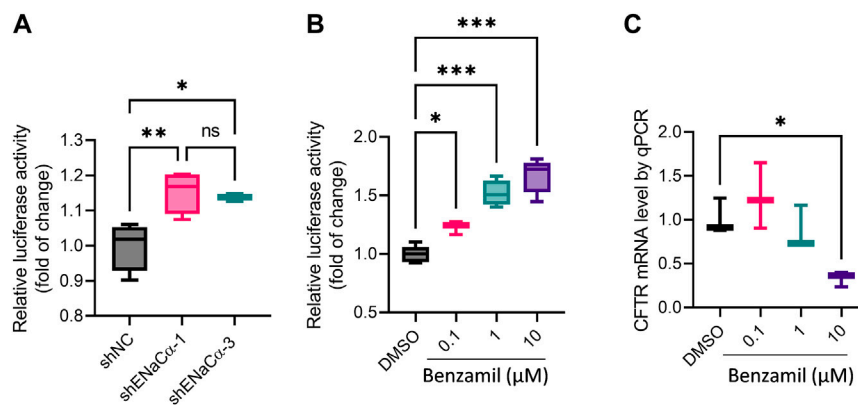


FIGURE 5 Effect of ENaC deficiency on CFTR transcription in ISK cells. (A–B) Measurement of CFTR transcription start by a dual luciferase reporter in ISK cells with shNC, shENaC-1 or shENaC-3 (A) or treated with benzamil (0.1–10 μM, 24 h). (B). (C) qPCR analysis of CFTR mRNA levels in ISK cells treated with benzamil (0.1–10 μM, 24 h). *N* = 4 (A), 3–6 (B) and 3 (C) **p* < 0.05, ****p* < 0.001, one-way ANOVA with *Dunnett post hoc* test.

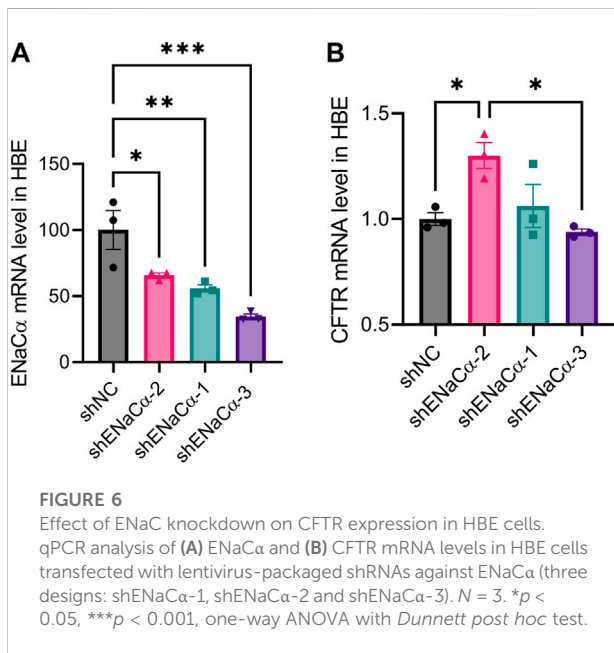


FIGURE 6 Effect of ENaC knockdown on CFTR expression in HBE cells. qPCR analysis of (A) ENaCα and (B) CFTR mRNA levels in HBE cells transfected with lentivirus-packaged shRNAs against ENaCα (three designs: shENaCα-1, shENaCα-2 and shENaCα-3). *N* = 3. **p* < 0.05, ****p* < 0.001, one-way ANOVA with *Dunnett post hoc* test.

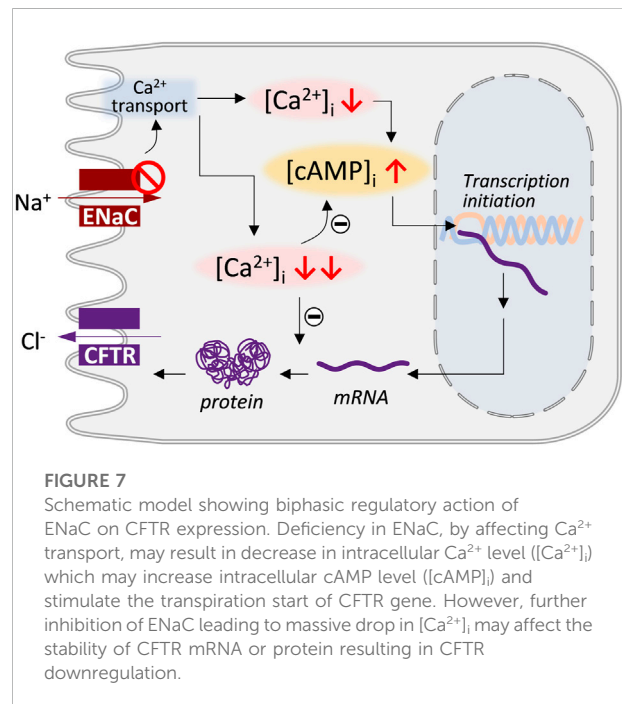


FIGURE 7 Schematic model showing biphasic regulatory action of ENaC on CFTR expression. Deficiency in ENaC, by affecting Ca²⁺ transport, may result in decrease in intracellular Ca²⁺ level ([Ca²⁺]_i) which may increase intracellular cAMP level ([cAMP]_i) and stimulate the transcription start of CFTR gene. However, further inhibition of ENaC leading to massive drop in [Ca²⁺]_i may affect the stability of CFTR mRNA or protein resulting in CFTR downregulation.

Discussion

In summary, the present study has demonstrated that CFTR functional expression in endometrial and airway epithelial cells may be subject to a biphasic regulation by ENaC (Figure 7). A low degree of ENaC deficiency may stimulate CFTR expression, while further attenuation of ENaC would not continue to increase but restore or even inhibit CFTR expression. Intracellular Ca²⁺-modulated sAC-driven cAMP production may be responsible for the positive regulation of CFTR by low-degree ENaC

deficiency. The negative regulation on CFTR expression by the high-degree ENaC deficiency might occur at post-transcription stages.

The interaction between CFTR and ENaC as two ion channels key to epithelial homeostasis has been noted for long (Kunzelmann, 2001; Berdiev et al., 2007; Berdiev et al., 2009; Gentzsch et al., 2010). Using electrophysiological approaches, most of the previous studies recognized a reciprocal relationship

between CFTR and ENaC channel open probability that when one is open the other tends to close or vice versa (Chan et al., 2000; Chan et al., 2001). Such a relationship is believed to be through quick protein-protein interactions (Kunzelmann, 2001; Berdiev et al., 2007; Gentzsch et al., 2010). Of note, gross ion channel activity is determined by both the open probability and plasma membrane density (or expression level) of the channel (Kashlan and Kleyman, 2011). The reciprocal relationship between the CFTR and ENaC was also observed at their expression levels, which was mostly seen in the female reproductive tract during menstrual cycle and believed to be a result of hormonal regulation (Chan et al., 2012). The present study has revealed that direct change in ENaC can affect CFTR gene transcription providing a mechanism how they interact at the expression level and in a relatively longer term. Moreover, such a regulatory effect on CFTR expression by ENaC is revealed to be not simply reciprocal but biphasic depending on the degree of ENaC deficiency. It therefore suggests the regulatory interaction between the two channels is far more complicated than originally thought, which may possibly explain why ENaC inhibitors failed to rescue CF airway (Graham et al., 1993; Pons et al., 2000; Hirsh et al., 2004), since a high degree of ENaC inhibition would not enhance CFTR but result in further CFTR deficiency. The degree of ENaC inhibition should be a key consideration for pharmaceutical design.

The present study also provides evidence that a cellular signaling pathway involving intracellular Ca^{2+} , sAC, and cAMP may underly the biphasic regulation of CFTR expression by ENaC. First, inhibition or knockdown of ENaC caused reduction in $[Ca^{2+}]_i$, while lowering intracellular Ca^{2+} by BAPTA-AM to different extents produced similar biphasic effect of ENaC knockdown on CFTR mRNA and cAMP levels. Second, inhibiting sAC by KH-7 abolished the biphasic effect of ENaC knockdown or BAPTA-AM. Of note, Ca^{2+} -activatable and inhibitable isoforms of mAC were identified to account for the dual role of Ca^{2+} in regulating cAMP levels (Antoni, 1997). However, the present data showed that mAC may not be essentially involved since the selective inhibition of mAC by DDA did not alter CFTR upregulation induced by ENaC knockdown or BAPTA-AM. Instead, sAC may be important here given the effect of KH-7 in abolishing ENaC knockdown or BAPTA-AM-induced CFTR upregulation. Although sAC has only been reported to be activated by Ca^{2+} (Jaiswal and Conti, 2003), dual role of Ca^{2+} in regulating cAMP levels was noted in sperm cells where sAC is well recognized to be essential to sperm cAMP production and thus sperm motility (Li et al., 2016). The present results suggest a possible inhibitory effect of Ca^{2+} on sAC in ISK cells too, which could be lifted by a low dose of BAPTA-AM or ENaC deficiency. The exact mechanism, however, awaits further investigation. Intriguingly, while the effects of ENaC knockdown on CFTR mRNA, protein and function levels

were biphasic depending on the knockdown degree, the luciferase reporter assay showed that all tested degrees of ENaC inhibition or knockdown stimulated CFTR transcription, suggesting that the negative regulation on CFTR expression by the high-degree ENaC deficiency might occur at post-transcription stages. It has been shown that Ca^{2+} participates in various signaling pathways that determine mRNA stability and thus protein expression (Misquitta et al., 2006). Possibly, massive reduction in Ca^{2+} as a result of high-degree ENaC deficiency reduced CFTR mRNA or protein stability in ISK cells (Figure 7). This may suggest that the biphasic relationship between ENaC and CFTR is a combined effect of transcription initiation and mRNA or protein stability reduction. The mechanisms underlying such a complex biphasic regulatory relationship will need to be further explored. Attention should be paid to the regulatory action of CFTR onto ENaC as well, given the recognized roles of CFTR in regulating multiple signaling pathways (Chen et al., 2012; Lu et al., 2012; Ruan et al., 2014; Dong et al., 2015; Sun et al., 2018a).

It should be noted that CFTR is presently shown to be only upregulated within a very small window (about 20%–30% ENaC deficiency) in the endometrial or bronchial epithelial cell models, suggesting a tight and complex regulation between ENaC and CFTR. Such a regulatory relationship should be of physiologically significant. In the endometrial epithelium, for an example, which undergoes dynamic changes and cyclic remodeling during the menstruation cycle, where ENaC and CFTR expressions are known to fluctuate (Ruan et al., 2014), the regulation between epithelial ion channels may provide an efficient mechanism for epithelial plasticity and self-remodeling. In other epithelial tissues such as the airway where the epithelial cells are subject to many environmental dynamics (e.g., airway pathogens), the tight regulation to realize the switch between secretion and absorption or other epithelial cell activities might also be of physiological or pathophysiological importance.

Materials and methods

Cell culture

Human endometrial epithelial cell line Ishikawa (ISK) was purchased from ATCC (Virginia, United States) and cultured in RPMI-1640 (Thermo Fisher, 31800022) supplemented with 10% fetal bovine serum (v/v) and 1% penicillin–streptomycin (v/v) in 5% CO_2 incubators at 37°C. The cell line was authenticated by STR profiling at the Department of Anatomical and Cellular Pathology, Faculty of Medicine, The Chinese University of Hong Kong. Human bronchial epithelial cell line (16HBE14o-, ATCC)

TABLE 1 ShRNA information.

	TRC no.	Sequence (from 5' to 3')	Predicted knockdown efficiency
shENaCa-1	TRCN0000044558	CCGGCCAGAACAAATCGGACTGCTTCTCGGAAGCAGTCCGATTTGTTCTGG TTTTTG	64
shENaCa-2	TRCN0000044562	CCGGCGCAGAGCAGAATGACTTCATCTCGAGATGAAGTCATTCTGCTCTGCGTT TTTG	78
shENaCa-3	TRCN0000044559	CCGGCGATGTATGGAAACTGCTATACTCGAGTATAGCAGTTCCATACATCGTT TTTG	95

TABLE 2 Primer list.

Gene	Forward	Reverse
Human ENaCa	AGCTCCTCCAGCTCCTCTTT	CAGCCTCAACATCAACCTCA
Human CFTR	GTGTGATTCACCTTCTCCAA	GCCTGGCACCATTAAAGAAA
Human GAPDH	AGGGTCATCATCTCTGCC	CCATCACGCCACAGTTTC

was a gift from Prof Zhou Wenliang at Sun Yat-sen University and cultured in Minimal Essential Medium (Thermo Fisher, 41500034) supplemented with 10% fetal bovine serum (v/v) and 1% penicillin–streptomycin (v/v) in 5% CO₂ incubators at 37°C.

ENaC knockdown

Three designs of shRNAs targeting ENaCa and the scrambled non-coding shRNAs (shNC) were purchased from (Sigma-Aldrich) (Table 1). To package the shRNAs into the lentivirus, envelope vector pMD2.G (Addgene, 12259), packaging vector psPAX2 (Addgene, 12260) and shRNAs together with lipofectamine 2000 (ThermoFisher Scientific) were transfected into 293FT cells. Packaged lentivirus was harvested 72 h after transfection and next transfected into ISK or HBE cells for 24 h in the presence of polybrene (6 µg/ml). The cells were then cultured in the presence of puromycin (1 µg/ml) for 14 days to achieve stable knockdown.

Quantitative PCR

Cells were lysed in TRIzol (Thermo Fisher Scientific, 15596026) for RNA extraction according to the manufacturer's instructions. 1 µg RNA was then reverse transcribed into cDNA using High-Capacity cDNA Reverse Transcription kit (Thermo Fisher Scientific, 4368814) following the manufacturer's instructions. Afterward, targeting genes (Table 2, all sequences were listed from 5' to 3') were amplified and detected by Touch Real-Time PCR Detection

System (Bio-Rad, CFX96) using STBR Green Master mix (TAKARA, RR420A). GAPDH was used as a housekeeping gene for normalization. The data were analyzed using $\Delta\Delta CT$ method.

Membrane potential imaging

Cells were seeded on coverslips and grown for 24 to 48 h before the experiment. Cells on the coverslip were washed off the growth medium with Margo-Ringer buffer (NaCl 130 mM, KCl 5 mM, MgCl₂ 1 mM, CaCl₂ 2.5 mM, Hepes 20 mM and glucose 10 mM, pH 7.4), mounted to a chamber containing 1 ml Margo-Ringer buffer with the presence of a membrane potential-sensitive fluorescence dye, DiBAC4(3) (1 µM, Thermo Fisher Scientific, B438) and then placed under a fluorescence microscope (Nikon, ECLIPSE Ti2). After 15 min stabilization, the DiBAC4(3) was excited at 488 nm with emission lights collected at 535 nm and pictures taken every 3–5 sec. The data were collected and analyzed through NIS-Elements software.

Western blot

Cells were lysed in pre-cooled RIPA lysis buffer (50 mM Tris-Cl, pH 7.5, 150 mM NaCl, 1% NP-40, 0.5% DOC and 0.1% SDS) with protease inhibitor cocktail (Thermo Fisher Scientific, 78443) for 30 min on ice. The supernatant was collected after centrifugation at 13,000 rpm for 30 min at 4°C. The protein concentration of each sample was measured with a BCA protein assay kit (Beyotime, P0011). Proteins were denatured

in LDS sample buffer (Thermo Fisher Scientific, NP0007) plus 4% β -mercaptoethanol (Acros, 125472500) with heating at 70°C for 10 min to detect ENaCa, or incubated at room temperature for 30 min to detect CFTR. After denaturation, proteins were separated by SDS-polyacrylamide gel electrophoresis and subsequently transferred to equilibrated nitrocellulose membrane. The membrane was blocked by 5% non-fat milk in TBS for 30 min and subsequently incubated with the primary antibody in 5% non-fat milk in TBS at 4°C overnight. Primary antibodies against CFTR (1:500, Alomone Labs, ACL-006), ENaCa (1:500, StressMarq, SPC403), and actin (1:2000, Sigma Aldrich, MAB1501R) were used. After three washes with 0.05% Tween 20 in TBS, the membrane was incubated with HRP-conjugated antibodies at room temperature for 1 h and visualized by ECL substrates (Bio-Rad, 170-5060) and ChemiDoc MP Imaging System (Bio-Rad). HRP-conjugated secondary antibodies were goat anti-rabbit IgG (1:2,000, Bio-Rad, 12004159) and goat anti-mouse IgG (1:2,000, Bio-Rad, 12004159). Image J software was used for the densitometry of western blots.

Intracellular Cl⁻ imaging

Cells were seeded on coverslips and grown for 24 to 48 h before the experiment. Prior to imaging, cells on the coverslip were incubated with a Cl⁻ sensitive fluorescent dye, MQAE (10 mM, MedChemExpress, HY-D0090) in Margo-Ringer buffer for 30 min at 37°C followed by washing and stabilizing for another 10 min. The coverslip was then mounted to a chamber containing 1 ml Margo-Ringer buffer under a fluorescence microscope (Nikon, ECLIPSE Ti2). MQAE was excited at 340 nm with emission at 460 nm every 3–5 sec. The data were collected and analyzed through NIS-Elements software.

Intracellular cAMP measurement

Intracellular cAMP concentration was measured with Direct cAMP ELISA Kit (Enzo Life Sciences, Cat. No. ADI-900-066). Cells were lysed with 0.1M HCl at room temperature for 10 min. The lysates were centrifuged at 1000 g for 5 min, and the supernatants were used for subsequent analysis. Part of the supernatants were used to determine protein concentration in each sample with BCA Protein Assay Kit (Beyotime, Cat No. P0011). Another part of the supernatants was used for cAMP measurement, added with acetylating reagent (10 μ l for every 200 μ l sample) to increase assay sensitivity. Sample wells, cAMP standard wells and other reference wells were loaded and treated according to assay layout sheet and product manual. Optical density

(OD) of each well was read at 405 nm with Ledetect 96 Absorbance Plate Reader (Labexim Products), subtracting mean OD of substrate blank from all measurements. Concentration of cAMP of each sample was calculated with a four-parameter logistic curve fitting program.

Ca²⁺ imaging and calibration

Cells seeded on coverslips were incubated with Fura-2 (2 μ M Thermo Fisher Scientific, F1221) for 30 min at 37°C before mounted onto a fluorescence microscope (Eclipse Ti, Nikon, Tokyo, and Japan). Fura-2 fluorescence was alternately excited at 340 and 380nm, and the emission signals were recorded at 510 nm. Ca²⁺ calibration was done according to a previous protocol (Williams and Fay, 1990). Briefly, cells were washed with Ca²⁺-free bath solution containing (in mM): NaCl 130, KCl 5, Hepes 20, EGTA 10 and glucose 10 (pH 7.2) before loaded with Fura-2 (2 μ M) in the bath solution at 37°C for 30 min. The coverslip was then transferred to a mini chamber containing 1 ml Ca²⁺-free bath solution supplemented with nigericin (5 μ M) and ionomycin (2 μ M), and mounted on to the fluorescence microscope. To calibrate the change in Fura-2 fluorescence intensity into Ca²⁺ concentrations, a series of volumes of a high Ca²⁺ buffer containing (in mM): NaCl 130, KCl 5, CaCl₂ 10, Hepes 20, EGTA 10 and glucose 10 (pH 7.2) supplemented with nigericin (5 μ M) and ionomycin (2 μ M) was added into the Ca²⁺-free bath to achieve CaEGTA concentrations at 0, 1, 2, 4, 6, 8, and 10 mM. The concentration of free Ca²⁺ was estimated using the equation: $[Ca^{2+}]_{free} = K_{d-EGTA} \times (C_{CaEGTA} / C_{K2EGTA})$, where K_{d-EGTA} is a constant of 150.5 at 20°C with a pH of 7.2. The calibration curve was obtained by fitting Fura-2 240/380 ratios with $[Ca^{2+}]_{free}$.

Luciferase activity assay

The proximal 5' region of human *CFTR* (- 1930 to +70, where +1 represents the transcriptional start site of *CFTR*) was amplified and cloned into pGL3-basic luciferase reporter by *KpnI* and *NheI* sites to make the pGL3/hCFTR construct (MiaoLingPlasmid Company). ISK cells were seeded into 96-well culture plates at a density of 1×10^4 cells/well and co-transfected with luciferase reporter plasmid (pGL3/hCFTR, 1,000 ng/well) and internal control plasmid (Renilla-Luc, 10 ng/well) using Lipofectamine 2000 (Invitrogen). Firefly and renilla luciferase activities were assessed using the Dual-Glo Luciferase Assay System (Promega, E2920) according to the manufacturer's instructions. The relative luciferase activity was defined as the ratio of readout for firefly luciferase to that for renilla

luciferase with that of control group set as 1.0. Triplicate wells were used for measurement at each group.

Statistics

One-way ANOVA was used for comparisons among more than 2 groups. Two-way ANOVA was used when there were two different categorical independent variables. A *p* value smaller than 0.05 was regarded as statistically significant. All graphs were generated and all statistical analyses were done with GraphPad Prism 9.

Data availability statement

The original contributions presented in the study are included in the article/supplementary material, further inquiries can be directed to the corresponding author.

Author contributions

Conception: YCR and FW. Experiments and/or data analysis: FW, XM, YQ, JC and YCR. Manuscript writing: YCR and FW with contributions by other co-authors.

References

- Anderson, M. P., Gregory, R. J., Thompson, S., Souza, D. W., Paul, S., Mulligan, R. C., et al. (1991). Demonstration that CFTR is a chloride channel by alteration of its anion selectivity. *Science* 253, 202–205. doi:10.1126/science.1712984
- Antoni, F. A. (1997). Calcium regulation of adenylyl cyclase relevance for endocrine control. *Trends Endocrinol. Metab.* 8, 7–14. doi:10.1016/s1043-2760(96)00206-8
- Berdiev, B. K., Cormet-Boyaka, E., Tousson, A., Qadri, Y. J., Oosterveld-Hut, H. M., Hong, J. S., et al. (2007). Molecular proximity of cystic fibrosis transmembrane conductance regulator and epithelial sodium channel assessed by fluorescence resonance energy transfer. *J. Biol. Chem.* 282, 36481–36488. doi:10.1074/jbc.M708089200
- Berdiev, B. K., Qadri, Y. J., and Benos, D. J. (2009). Assessment of the CFTR and ENaC association. *Mol. Biosyst.* 5, 123–127. doi:10.1039/b810471a
- Canessa, C. M., Schild, L., Buell, G., Thorens, B., Gautschi, I., Horisberger, J. D., et al. (1994). Amiloride-sensitive epithelial Na⁺ channel is made of three homologous subunits. *Nature* 367, 463–467. doi:10.1038/367463a0
- Chan, L. N., Wang, X. F., Tsang, L. L., So, S. C., Chung, Y. W., Liu, C. Q., et al. (2001). Inhibition of amiloride-sensitive Na⁺ absorption by activation of CFTR in mouse endometrial epithelium. *Pflugers Arch.* 443 (Suppl. 1), S132–S136. doi:10.1007/s004240100660
- Chan, H. C., Chen, H., Ruan, Y., and Sun, T. (2012). Physiology and pathophysiology of the epithelial barrier of the female reproductive tract: role of ion channels. *Adv. Exp. Med. Biol.* 763, 193–217. doi:10.1007/978-1-4614-4711-5_10
- Chan, H. C., Ruan, Y. C., He, Q., Chen, M. H., Chen, H., Xu, W. M., et al. (2009). The cystic fibrosis transmembrane conductance regulator in reproductive health and disease. *J. Physiol.* 587, 2187–2195. doi:10.1113/jphysiol.2008.164970
- Chan, L. N., Wang, X. F., Tsang, L. L., Liu, C. Q., and Chan, H. C. (2000). Suppression of CFTR-mediated Cl⁻ secretion by enhanced expression of epithelial Na⁺ channels in mouse endometrial epithelium. *Biochem. Biophys. Res. Commun.* 276, 40–44. doi:10.1006/bbrc.2000.3426
- Chen, H., Ruan, Y. C., Xu, W. M., Chen, J., and Chan, H. C. (2012). Regulation of male fertility by CFTR and implications in male infertility. *Hum. Reprod. Update* 18, 703–713. doi:10.1093/humupd/dms027
- Cheng, S. H., Rich, D. P., Marshall, J., Gregory, R. J., Welsh, M. J., and Smith, A. E. (1991). Phosphorylation of the R domain by cAMP-dependent protein kinase regulates the CFTR chloride channel. *Cell* 66, 1027–1036. doi:10.1016/0092-8674(91)90446-6
- Dagenais, A., Denis, C., Vives, M. F., Girouard, S., Masse, C., Nguyen, T., et al. (2001). Modulation of alpha-ENaC and alpha1-Na⁺-K⁺-ATPase by cAMP and dexamethasone in alveolar epithelial cells. *Am. J. Physiol. Lung Cell. Mol. Physiol.* 281, L217–L230. doi:10.1152/ajplung.2001.281.1.L217
- Dagenais, A., Desjardins, J., Shabbir, W., Roy, A., Filion, D., Sauve, R., et al. (2018). Loss of barrier integrity in alveolar epithelial cells downregulates ENaC expression and activity via Ca(2+) and TRPV4 activation. *Pflugers Arch.* 470, 1615–1631. doi:10.1007/s00424-018-2182-4
- Dong, Z. W., Chen, J., Ruan, Y. C., Zhou, T., Chen, Y., Chen, Y., et al. (2015). CFTR-regulated MAPK/NF-kappaB signaling in pulmonary inflammation in thermal inhalation injury. *Sci. Rep.* 5, 15946. doi:10.1038/srep15946
- Fei, Y., Sun, L., Yuan, C., Jiang, M., Lou, Q., and Xu, Y. (2018). CFTR ameliorates high glucose-induced oxidative stress and inflammation by mediating the NF-kappaB and MAPK signaling pathways in endothelial cells. *Int. J. Mol. Med.* 41, 3501–3508. doi:10.3892/ijmm.2018.3547
- Genzsch, M., Dang, H., Dang, Y., Garcia-Caballero, A., Suchindran, H., Boucher, R. C., et al. (2010). The cystic fibrosis transmembrane conductance regulator impedes proteolytic stimulation of the epithelial Na⁺ channel. *J. Biol. Chem.* 285, 32227–32232. doi:10.1074/jbc.M110.155259
- Graham, A., Hasani, A., Alton, E. W., Martin, G. P., Marriot, C., Hodson, M. E., et al. (1993). No added benefit from nebulized amiloride in patients with cystic fibrosis. *Eur. Respir. J.* 6, 1243–1248.
- Irsh, A. J., Sabater, J. R., Zamurs, A., Smith, R. T., Paradiso, A. M., Hopkins, S., et al. (2004). Evaluation of second generation amiloride analogs as therapy for cystic

Funding

The work was supported in part by National Natural Science Foundation of China (No. 82071599), Early Career Scheme of Hong Kong (No. 24104517), Theme-based Research Scheme of Hong Kong (No. T13-402/17N), Areas of Excellence Scheme of Hong Kong (AoE/M-402/20), Health and Medical Research Fund of Hong Kong (No. 18191361) and Start-up fund at the Hong Kong Polytechnic University.

Conflict of interest

The authors declare that the research was conducted in the absence of any commercial or financial relationships that could be construed as a potential conflict of interest.

Publisher's note

All claims expressed in this article are solely those of the authors and do not necessarily represent those of their affiliated organizations, or those of the publisher, the editors and the reviewers. Any product that may be evaluated in this article, or claim that may be made by its manufacturer, is not guaranteed or endorsed by the publisher.

- fibrosis lung disease. *J. Pharmacol. Exp. Ther.* 311, 929–938. doi:10.1124/jpet.104.071886
- Hobbs, C. A., Da Tan, C., and Tarran, R. (2013). Does epithelial sodium channel hyperactivity contribute to cystic fibrosis lung disease? *J. Physiol.* 591, 4377–4387. doi:10.1113/jphysiol.2012.240861
- Jaiswal, B. S., and Conti, M. (2003). Calcium regulation of the soluble adenylyl cyclase expressed in mammalian spermatozoa. *Proc. Natl. Acad. Sci. U. S. A.* 100, 10676–10681. doi:10.1073/pnas.1831008100
- Kashlan, O. B., and Kleyman, T. R. (2011). ENaC structure and function in the wake of a resolved structure of a family member. *Am. J. Physiol. Ren. Physiol.* 301, F684–F696. doi:10.1152/ajprenal.00259.2011
- Konig, J., Schreiber, R., Voelcker, T., Mall, M., and Kunzelmann, K. (2001). The cystic fibrosis transmembrane conductance regulator (CFTR) inhibits ENaC through an increase in the intracellular Cl⁻ concentration. *EMBO Rep.* 2, 1047–1051. doi:10.1093/embo-reports/kve232
- Kunzelmann, K. (2001). CFTR: interacting with everything? *News Physiol. Sci.* 16, 167–170. doi:10.1152/physiologyonline.2001.16.4.167
- Li, X., Wang, L., Li, Y., Zhao, N., Zhen, L., Fu, J., et al. (2016). Calcium regulates motility and protein phosphorylation by changing cAMP and ATP concentrations in boar sperm *in vitro*. *Anim. Reprod. Sci.* 172, 39–51. doi:10.1016/j.anireprosci.2016.07.001
- Lu, Y. C., Chen, H., Fok, K. L., Tsang, L. L., Yu, M. K., Zhang, X. H., et al. (2012). CFTR mediates bicarbonate-dependent activation of miR-125b in preimplantation embryo development. *Cell Res.* 22, 1453–1466. doi:10.1038/cr.2012.88
- Madacsy, T., Pallagi, P., and Maleth, J. (2018). Cystic fibrosis of the pancreas: the role of CFTR channel in the regulation of intracellular Ca²⁺ signaling and mitochondrial function in the exocrine pancreas. *Front. Physiol.* 9, 1585. doi:10.3389/fphys.2018.01585
- McCarthy, V. A., and Harris, A. (2005). The CFTR gene and regulation of its expression. *Pediatr. Pulmonol.* 40, 1–8. doi:10.1002/ppul.20199
- Misquitta, C. M., Chen, T., and Grover, A. K. (2006). Control of protein expression through mRNA stability in calcium signalling. *Cell Calcium* 40, 329–346. doi:10.1016/j.ceca.2006.04.004
- Nishida, M. (2002). The Ishikawa cells from birth to the present. *Hum. Cell* 15, 104–117. doi:10.1111/j.1749-0774.2002.tb00105.x
- Palmer, L. G. (1992). Epithelial Na channels: function and diversity. *Annu. Rev. Physiol.* 54, 51–66. doi:10.1146/annurev.ph.54.030192.000411
- Pons, G., Marchand, M. C., d'Athis, P., Sauvage, E., Foucard, C., Chaumet-Riffaud, P., et al. (2000). French multicenter randomized double-blind placebo-controlled trial on nebulized amiloride in cystic fibrosis patients. The Amiloride-AFLM Collaborative Study Group. *Pediatr. Pulmonol.* 30, 25–31. doi:10.1002/1099-0496(200007)30:1<25::aid-ppul5>3.0.co;2-c
- Reddy, M. M., Light, M. J., and Quinton, P. M. (1999). Activation of the epithelial Na⁺ channel (ENaC) requires CFTR Cl⁻ channel function. *Nature* 402, 301–304. doi:10.1038/46297
- Reddy, M. M., and Quinton, P. M. (2003). Functional interaction of CFTR and ENaC in sweat glands. *Pflugers Arch.* 445, 499–503. doi:10.1007/s00424-002-0959-x
- Ruan, Y. C., Chen, H., and Chan, H. C. (2014). Ion channels in the endometrium: regulation of endometrial receptivity and embryo implantation. *Hum. Reprod. Update* 20, 517–529. doi:10.1093/humupd/dmu006
- Ruan, Y. C., Guo, J. H., Liu, X., Zhang, R., Tsang, L. L., Dong, J. D., et al. (2012). Activation of the epithelial Na⁺ channel triggers prostaglandin E(2) release and production required for embryo implantation. *Nat. Med.* 18, 1112–1117. doi:10.1038/nm.2771
- Sun, H., Wang, Y., Zhang, J., Chen, Y., Liu, Y., Lin, Z., et al. (2018a). CFTR mutation enhances Dishevelled degradation and results in impairment of Wnt-dependent hematopoiesis. *Cell Death Dis.* 9, 275. doi:10.1038/s41419-018-0311-9
- Sun, X., Guo, J. H., Zhang, D., Chen, J. J., Lin, W. Y., Huang, Y., et al. (2018b). Activation of the epithelial sodium channel (ENaC) leads to cytokine profile shift to pro-inflammatory in labor. *EMBO Mol. Med.* 10. doi:10.15252/emmm.201808868
- Sun, X., Ruan, Y. C., Guo, J., Chen, H., Tsang, L. L., Zhang, X., et al. (2014). Regulation of miR-101/miR-199a-3p by the epithelial sodium channel during embryo implantation: involvement of CREB phosphorylation. *Reproduction* 148, 559–568. doi:10.1530/REP-14-0386
- Williams, D., and Fay, F. (1990). Intracellular calibration of the fluorescent calcium indicator Fura-2. *Cell Calcium* 11, 75–83. doi:10.1016/0143-4160(90)90061-x